Spin Disorder and Order in Quasi-2D Triangular Heisenberg Antiferromagnets: Comparative Study of $FeGa_2S_4$, $Fe_2Ga_2S_5$, and $NiGa_2S_4$

S. Nakatsuji,[1,2] H. Tonomura,[1] K. Onuma,[1] Y. Nambu,[1,2] O. Sakai,[1] Y. Maeno,[1] R. T. Macaluso,[3] and Julia Y. Chan[3]

[1]*Department of Physics, Kyoto University, Kyoto 606-8502, Japan*

[2]*Institute for Solid State Physics, University of Tokyo, Kashiwa, 277-8581, Japan*

[3]*Department of Chemistry, Louisiana State University, Baton Rouge, Louisiana 70803, USA*

(Received 21 January 2007; revised manuscript received 11 July 2007; published 11 October 2007)

Our single crystal study reveals that the single-layer $S = 2$ triangular Heisenberg antiferromagnet $FeGa_2S_4$ forms a frozen spin-disordered state, similar to the $S = 1$ isostructural magnet $NiGa_2S_4$. In this state, the magnetic specific heat C_M is not only insensitive to the field, but shows a T^2 dependence that scales to C_M of $NiGa_2S_4$, suggesting the same underlying mechanism of the 2D coherent behavior. In contrast, the bilayer system $Fe_2Ga_2S_5$ exhibits a 3D antiferromagnetic order.

DOI: 10.1103/PhysRevLett.99.157203 PACS numbers: 75.40.Cx, 75.50.Bb, 75.50.Ee

Geometrically frustrated magnets have attracted great interest for the possible emergence of novel spin-disordered states such as spin liquid and glass. In two dimensions (2D), the triangular lattice is the simplest form of a geometrically frustrated lattice with a single magnetic ion in a unit cell, and has been extensively studied to search for spin-disordered states [1]. $NiGa_2S_4$ is a rare example of low spin antiferromagnets (AFMs) on an exact triangular lattice [2]. Despite a strong antiferromagnetic (AF) coupling with the Weiss temperature $\theta_W = 80$ K, no AF or canonical spin glass ordering has been observed down to 0.35 K. Instead, below $T_f = 10\ \text{K} \sim \theta_W/10$ it develops a short-range noncollinear order with 2D gapless linearly dispersive excitations characterized by a T^2 dependence of the specific heat [2,3]. Recent nuclear-quadrupole-resonance and muon-spin-relaxation measurements have revealed that the internal fields set in below 10 K with a strong divergence of the relaxation rate $1/T_1$. Moreover, the divergence occurs over a wide T range down to 2 K. These indicate that spins become gradually frozen below T_f, and retain critical fluctuations even far below T_f [4].

Outstanding questions are the origin and stability of the 2D coherent behavior in the spin-disordered state. In this regard, various theoretical proposals have been made [5–10]. Experimentally, it is highly important to study the effect of spin size change, bilayering, and geometrical frustration, and to see if any spin order can be realized in the related compounds. Here, we report the single crystal study of the isostructural single-layer triangular AFMs, $NiGa_2S_4$ and $FeGa_2S_4$, and the homologous bilayer triangular AFM $Fe_2Ga_2S_5$. For $NiGa_2S_4$, we have succeeded in growing single crystals for the first time and found properties fully consistent with those for polycrystalline samples [11]. Strikingly, the magnetic properties of $FeGa_2S_4$ bear strong resemblances to those of $NiGa_2S_4$ despite the fact that Fe^{2+} has twice larger $S = 2$ spin than $S = 1$ for Ni^{2+}. Both compounds have basically Heisenberg spins, and form frozen disordered state below $T \sim \theta_W/10$. In addition, the low T specific heat is insensitive to the field and shows a T^2 dependence, which scales to that of $NiGa_2S_4$. The similarities strongly suggest that the 2D coherent behavior in the frozen spin-disordered state has the same underlying mechanism. In contrast, a clear AF transition is observed for the bilayer system $Fe_2Ga_2S_5$, whose dominant AF bonds most likely form an unfrustrated honeycomb lattice. These results suggest that the geometrical frustration of the single-layer triangular lattices stabilizes the spin-disordered state, probably associated with 2D AF ordering.

Single crystals were grown by chemical-vapor transport using iodine [11–13]. Powder and single crystal x-ray diffraction confirmed sample homogeneity and structure. We measured d.c. susceptibility χ down to 1.8 K with a SQUID magnetometer, and specific heat C_P down to 0.35 K using a thermal relaxation method.

AGa_2S_4 (A = Ni, Fe) and $Fe_2Ga_2S_5$ are layered chalcogenide insulators with triangular lattices (Fig. 1) [2,12,13]. The structure of AGa_2S_4 can be described in terms of slabs consisting of two GaS layers and one AS_2 layer, stacked along the c axis and separated by a van der Waals gap. The central AS_2 layer is isostructural with the CoO_2 layer of the superconductor $Na_xCoO_2 \cdot yH_2O$ [14]. $Fe_2Ga_2S_5$ has a bilayer version of $FeGa_2S_4$ structure: a Fe_2S_3 layer consisting of a pair of triangular planes of Fe^{2+} replaces the central FeS_2 layer of $FeGa_2S_4$.

Ni^{2+} of $NiGa_2S_4$ has the configuration of $t_{2g}^6 e_g^2$ with no orbital degree of freedom, and its $S = 1$ spin should be of the Heisenberg type. For $FeGa_2S_4$ and $Fe_2Ga_2S_5$, Fe^{2+} has the $t_{2g}^4 e_g^2$ configuration with high spin $S = 2$, and thus Jahn-Teller (JT) active. A weak rhombohedral distortion of each FeS_6 octahedron should split the t_{2g} orbitals and stabilize one a_{1g} level against two e_g levels by a JT gap Δ_{JT}, which should be of the order of 300 K similar to what was calculated for the isostructural CoO_2 layer [15]. Thus, the ground state has no orbital degree of freedom, and the spins should be of Heisenberg type.

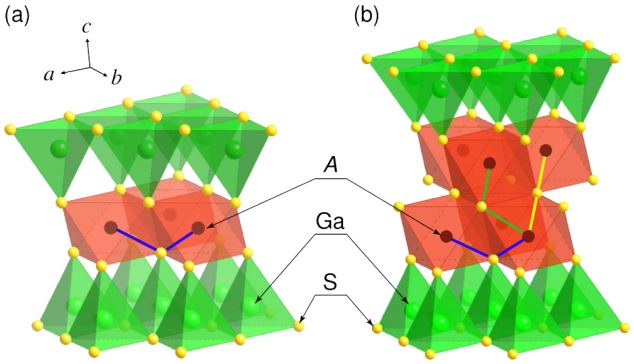

FIG. 1 (color online). Structure of the unit slab for (a) single layered AGa_2S_4 (A = Ni, Fe) and (b) bilayer $Fe_2Ga_2S_5$. Superexchange paths are shown by lines within the diagrams (color online).

Notably, all compounds have the same interslab structure including the van der Waals gap, which should significantly weaken the c-axis coupling. In addition, the Ni/Fe in the nearest neighbor in different slabs are separated by similar distances 11.999, 12.056 Å (Ni, Fe single layer) and 11.928 Å (Fe bilayer), more than 3 times longer than the in-plane Ni/Fe distances given by the lattice parameters $a = 3.624$, 3.654 Å (Ni, Fe single layer) and $a = 3.651$ Å (Fe bilayer). Thus for the all compounds, the effective dimensionality must be the same and quasi-2D.

A major difference in the crystal structures is the presence of the interlayer bonds for the bilayer compound. In addition to the intralayer couplings that form the triangular lattice of the single-layer [e.g., nearest neighbor (NN) bonds with nearly rectangular A-S-A path denoted by dark gray lines (blue online) connecting A and S molecules near the middle of each structure in Fig. 1(a)], the bilayer $Fe_2Ga_2S_5$ has the interlayer couplings that have two major Fe-S-Fe *inter* layer paths: (1) nearly rectangular (~90.5°) paths between the NN Fe sites [medium gray lines (green online) in Fig. 1(b)], (2) 180° paths connecting the second nearest neighbors [light gray line (yellow online) in Fig. 1(b)]. According to the Kanamori-Goodenough rule, the superexchange coupling through the latter straight Fe-S-Fe path (light gray/yellow) must be AF and much stronger than the other nearly rectangular NN couplings (dark and medium gray/blue and green) and longer range interactions [16]. Interestingly, this dominant AF bond forms four sublattices of a buckled *honeycomb lattice* in the bilayer [Fig. 2(a)]. Unlike the triangular lattice, the honeycomb lattice is bipartite, and its Heisenberg model with $S > 3/2$ is not frustrated but has Néel order [17]. Thus, the effective spin lattice of the bilayer system may well be the unfrustrated honeycomb lattice formed by the straight interlayer couplings.

Differences in the spin lattice strongly affect the magnetism, as can be seen in the T dependence of the susceptibility $\chi(T)$ [see Figs. 2(b) and 2(c)]. $NiGa_2S_4$ shows highly isotropic behavior. The Curie-Weiss (CW) fitting at $T > 100$ K, using the formula $\chi(T) = \chi_0 + C/(T + \theta_W)$, yields results fully consistent with those for polycrystalline samples, $\chi_0 \sim 0$, $p_{\text{eff}} = 2.86(2)\mu_B$ close to the expected value $2.83\mu_B$ for $S = 1$, and AF Weiss temperature θ_W of 80(2) K for both ab plane and c axis. The ab plane $\chi(T)$ shows a broad peak around $T_f = 10$ K.

$FeGa_2S_4$ also shows nearly isotropic behavior at $T > 250$ K, where the CW fitting yields $\chi_0 \sim 2 \times 10^{-4}$ emu/mole-Fe and the isotropic effective moments $p_{\text{eff}} = 5.45(5)\mu_B$ along the [100], [120], and [001] axes. The isotropy is consistent with the expectation that all the t_{2g} orbitals should be nearly equally populated at $T > \Delta_{\text{JT}} \sim 300$ K. In addition, the values of p_{eff} include a slight orbital component as well as $S = 2$ spin contribution ($p_{\text{eff}} = 4.90\mu_B$) as normally observed for Fe^{2+}. θ_W is AF and 160(9) K for all axes. On cooling, $\chi(T)$ develops weak easy-plane anisotropy, but not in-plane anisotropy. Finally, at $T_f = 16$ K $\sim \theta_W/10$, $\chi(T)$ shows a kink and a bifurcation between the field-cooled (FC) and zero-field-cooled (ZFC) results for all axes. Notably, the difference between FC and ZFC components at 1.8 K amounts to 30–50% of the total χ, much more than 6% seen for the $NiGa_2S_4$ case [2,11]. Anisotropy χ_{ab}/χ_c increases on cooling from the unity but reaches only 1.3 in the frozen

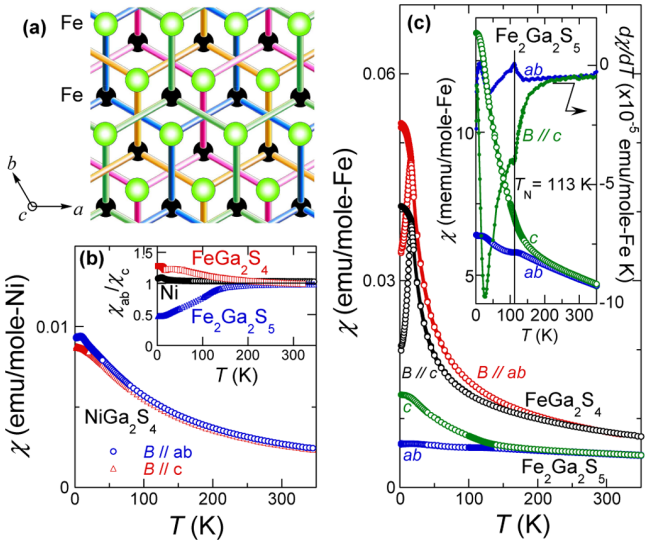

FIG. 2 (color online). (a) Four sublattices (in different colors online) of the buckled honeycomb lattice formed by the Fe-S-Fe straight bonds [yellow path online in Fig. 1(b)] in the bilayer of $Fe_2Ga_2S_5$. The Fe atoms in the upper triangular lattice layer of the bilayer are shown by open spheres (green online), while the ones in the lower layer by solid black. (b), (c) ab plane and c-axis components of $\chi(T)$ for (b) $NiGa_2S_4$ under $B = 7$ T, (c) $FeGa_2S_4$ and $Fe_2Ga_2S_5$ under $B = 0.1$ T. Both FC (solid symbol) and ZFC results (open symbol) are shown. No in-plane anisotropy was found. Insets: (b) Anisotropy $\chi_{ab}/\chi_c(T)$ obtained in the FC sequence for $NiGa_2S_4$ (circles), $FeGa_2S_4$ (squares) and $Fe_2Ga_2S_5$ (triangles). The horizontal line indicates the unity for the isotropic case. (c) $\chi(T)$ and $d\chi(T)/dT$ of $Fe_2Ga_2S_5$. The vertical lines indicate the Néel point T_N.

state [inset of Fig. 2(b)]. This indicates that the Fe^{2+} $S = 2$ spins are of Heisenberg type with weak easy-plane anisotropy, similar to $NiGa_2S_4$, where χ_{ab}/χ_c is more isotropic, but still larger than 1 [inset of Fig. 2(b)] [11].

For $Fe_2Ga_2S_5$, $\chi(T)$ is much more suppressed, suggesting a strong AF coupling. Above 200 K, all components follow the CW law, and the analysis yields $\chi_0 \sim 1 \times 10^{-3}$ emu/mole-Fe and the isotropic $p_{\text{eff}} = 5.00(7)\mu_B$, slightly smaller than the single-layer case. θ_{W} is indeed strongly AF and 540(3) K for [100], [120], and 480(3) K for [001]. The large enhancement in θ_{W} in comparison with the single layered materials is ascribable to the existence of the straight Fe-S-Fe interlayer bonds in the bilayer. Below 150 K, the ab plane and c-axis susceptibilities exhibit clear anisotropy. Moreover, a plateau with a cusp is found for ab plane around 113 K, while the c axis $\chi(T)$ shows a significant increase on cooling [inset of Fig. 2(c)]. The temperature derivative, $d\chi/dT$, on the other hand, reveals the anomalies at 113 K as kinks for both axes [inset of Fig. 2(c)]. Given no glassy hysteresis between the FC and ZFC results and the corresponding specific heat peak anomaly described below, it is an AF long-range order (LRO) that takes place at $T_{\text{N}} = 113$ K. This is consistent with the expectation that the effective honeycomb lattice of the bilayer is unfrustrated and thus should form an AF order. Above T_{N}, χ_{ab}/χ_c is slightly smaller than 1, indicating that spins are of Heisenberg type with slight Ising anisotropy.

Different behavior for the single and bilayer Fe sulfides is also observed in the specific heat results [Fig. 3(a)]. C_P/T of $FeGa_2S_4$ only shows a smooth change down to 0.35 K well below $\theta_{\text{W}} = 160$ K. This indicates that the system does not exhibit any LRO and thus the spins remain disordered. In contrast, C_P/T for $Fe_2Ga_2S_5$ yields a weak, but a clear cusplike anomaly at $T_{\text{N}} = 113$ K, which confirms the thermodynamic AF transition as suggested by the above susceptibility results.

In order to estimate the lattice part of the specific heat C_{L} for (Ni, Fe)Ga_2S_4 and $Fe_2Ga_2S_5$, we measured C_P of their nonmagnetic, isostructural analogues $ZnIn_2S_4$ and $Zn_2In_2S_5$, respectively, and followed the same conversion procedure using the Debye equation as the one described in Ref. [2]. The magnetic part of the specific heat divided by T, C_{M}/T, is thus obtained by subtracting C_{L}/T from C_P/T [Figs. 3(a) and 3(b)]. The results of single crystal $NiGa_2S_4$ are consistent with the ones for polycrystalline samples [Fig. 4(a)] [2,11]. Similar to $NiGa_2S_4$, $FeGa_2S_4$ exhibits a double-peak structure of C_{M}/T: one at ~10 K, and the other ~60 K. The lower temperature peak appears close to the freezing anomaly of $\chi(T)$ at $T_f = 16$ K, and is probably associated with the spin freezing. The entropy S_{M} estimated by the integration of C_{M}/T reaches $R\ln(5)$ corresponding to the $S = 2$ spin degree of freedom at $T \sim 100$ K, and gradually saturates toward $R\ln(15) = R\ln(5) + R\ln(3)$ [Fig. 3(b), right axis]. The latter $R\ln(3)$ gives the orbital degree of freedom due to two holes in the t_{2g} orbitals. The observed thermal excitation in the t_{2g} orbitals at $T > 100$ K is consistent with the estimated $\Delta_{\text{JT}} \sim 300$ K. Given $\theta_W = 160$ K, the broad feature of the higher T peak should also reflect the development of AF short-range order below $T \sim \theta_{\text{W}}$.

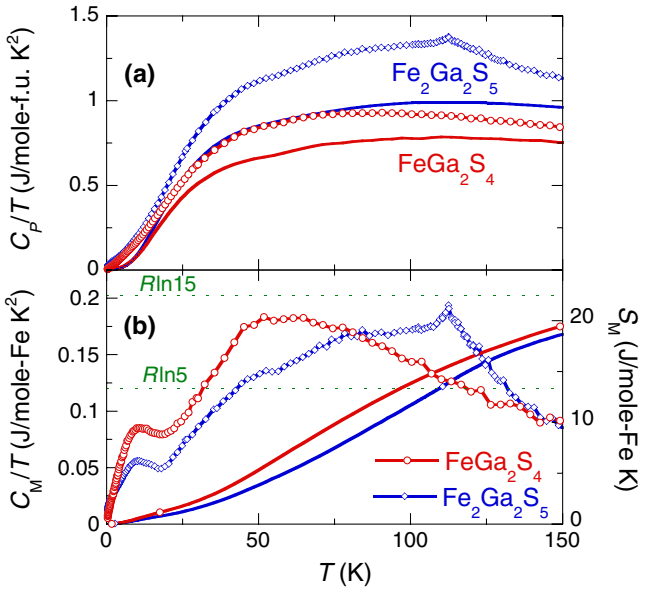

FIG. 3 (color online). (a) Total specific heat divided by temperature C_P/T, and their lattice contribution C_{L}/T (solid line), (b) magnetic part of the specific heat divided by temperature C_{M}/T (left axis), the entropy S_{M} (right axis) for $FeGa_2S_4$ (circle) and for $Fe_2Ga_2S_5$ (diamond). The horizontal broken lines indicate $S_{\text{M}} = R\ln5$ and $R\ln15$.

For $Fe_2Ga_2S_5$, C_{M}/T reveals a clear sharp peak at $T_{\text{N}} = 113$ K due to the AF-LRO. However, the corresponding entropy anomaly is weak, indicating the strong spin fluctuations due to the quasi two-dimensionality. Interestingly, C_{M}/T shows another broad peak at 10 K, corresponding to the formation of the plateau in $\chi(T)$.

To characterize spin excitations in the frozen spin-disordered state of the single layered compounds, we measured the low T specific heat under fields up to 7 T. Strikingly, little field response is observed in C_{M}/T for $FeGa_2S_4$ as well as $NiGa_2S_4$ [see Figs. 4(a) and 4(b)]. Generally, the external field, $B_c \sim k_B T_f/g\mu_B S$, fully polarizes individual spins of spin glasses, and strongly reduces C_{M}/T by opening the Zeeman gap in the spin excitation spectrum. In contrast, the observed no change in the low T limit under the estimated $B_c \sim 7$ T ($NiGa_2S_4$), 6 T ($FeGa_2S_4$), and above indicates that the elementary spin excitations are insensitive to the field.

Remarkably, the low T part of $C_{\text{M}}(T)$ of the single layered materials shows a T^2 dependence, indicating gapless linearly dispersive modes in 2D. Figs. 4(a) and 4(b) present the T-linear dependence of C_{M}/T over a decade of T between 0.35 K and 4.0 K for (Ni, Fe)Ga_2S_4. A distinct difference is a finite value of 3.1(1) mJ/mole K^2 for $\gamma \equiv C_{\text{M}}/T$ at $T \to 0$ K for $FeGa_2S_4$, whereas $\gamma = 0.0(1)$ mJ/mole K^2 for $NiGa_2S_4$ [2]. The T^2 dependence

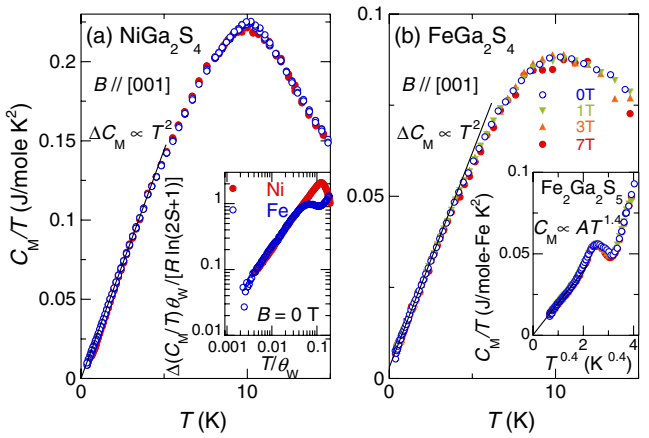

FIG. 4 (color online). Power law behavior of C_M/T for (a) $NiGa_2S_4$, (b) $FeGa_2S_4$, inset of (b) $Fe_2Ga_2S_5$ under various fields along the c axis. Inset of (a): $\Delta(C_M/T)\theta_W/[R\ln(2S+1)]$ vs T/θ_W for $NiGa_2S_4(S=1, \theta_W = 80\ \mathrm{K})$ and $FeGa_2S_4(S=2, \theta_W = 160\ \mathrm{K})$ at 0 T in full logarithmic scale.

without a magnetic LRO implies relatively long coherence length for the 2D modes that propagate through the spin-disordered state. This is in sharp contrast with local fluctuations in spin glasses that generate the T linear $C_M(T)$.

With 2D gapless linearly dispersive modes, the specific heat has the low-T asymptotic form as $C_M/R = (3\sqrt{3}\zeta(3)/2\pi)(ak_BT/\hbar D)^2$, where $\zeta(3) = 1.202$ [2]. For ordinary AFMs that order at $T \sim \theta_W$, the stiffness D is estimated by $D^2 \approx (3\sqrt{3}\zeta(3)/4\pi)(ak_B\theta_W/\hbar)^2/\ln(2S+1)$. For $NiGa_2S_4$ ($FeGa_2S_4$), the observed D is 850 (1300) m/s, ~3 times smaller than $D \approx 2500(4200)$ m/s estimated by this equation, indicating softening due to magnetic frustration. As suggested by the above equations, when $\Delta(C_M/T)\theta_W/[R\ln(2S+1)]$ is plotted vs T/θ_W [Fig. 4(a) inset]with $\Delta(C_M/T) \equiv C_M/T - \gamma$, the low T data for $FeGa_2S_4$ collapse on top of the one for $NiGa_2S_4$.

The experiments reported here reveal striking resemblances of the two isostructural compounds: (i) Heisenberg spins, (ii) frozen spin-disordered states below $T \sim \theta_W/10$, and (iii) field insensitivity and the scaling of the T^2-dependent specific heat in the disordered states. These results strongly suggest that the 2D coherent behavior of the two compounds has the same underlying mechanism.

Given almost the same dimensionality for all compounds, the 3D LRO in $Fe_2Ga_2S_5$ indicates that there exists a small but finite coupling along the c axis even in (Ni, Fe)Ga_2S_4. Nevertheless, both compounds exhibit the robust 2D coherent behavior: T^2-dependent C_M and its scaling with θ_W, whose dominant contribution comes from the in-plane coupling. These indicate that the spin-disordered state is a strongly 2D state stabilized by the frustrated AF in-plane coupling, not by the c-axis one.

Two types of theoretical proposals have been made for the origin of the disordered state and 2D coherent behavior in $NiGa_2S_4$ [5–10]. One is related to the ferro or antiferro spin nematic states in which spin quadrupoles, not ordinary dipoles, form a LRO [5–8]. While the frozen states of Ni and Fe compounds are not canonical spin glasses, they are not simply compatible with the nematic states. The other involves the nearly critical state associated with a 2D noncollinear AF order [9,10]. In this case, recent theory considers Z_2 vortices due to the noncollinear spin structure and predicts that their condensation at a finite T leads to a significant slowing down of spin dynamics and stabilizes a nearly critical state [10]. This may explain the 2D coherent behavior and glassy dynamics of the spin-disordered states in (Ni, Fe)Ga_2S_4 [4]. The pronounced freezing behavior of the $S = 2$ Fe system such as large hysteresis in $\chi(T)$ and a finite γ probably comes from its stronger classical-spin characteristics than the $S = 1$ case of $NiGa_2S_4$.

Finally, in the bilayer system, $C_M(T)$ shows $T^{1.4}$ behavior over a decade of T between 0.35 K and 3.8 K, and has little response to fields up to 7 T [Inset of Fig. 4(b)]. For a 3D AF-LRO as found in $Fe_2Ga_2S_5$, C_M is expected to exhibit the T^3 law. The $T^{1.4}$ dependence is, thus, unusual and an interesting subject for future studies.

We thank K. Ishida, H. Tsunetsugu, S. Fujimoto, and H. Kawamura for useful discussions. This work has been supported in part by Grants-in-Aids for Scientific Research from JSPS and for the 21st Century COE "Center for Diversity and Universality in Physics" from MEXT of Japan. J. Y. C. acknowledges the NSF (No. DMR 0237664) and the Alfred P. Sloan Foundation for support.

[1] M. F. Collins and O. A. Petrenko, Can. J. Phys. **75**, 605 (1997).
[2] S. Nakatsuji *et al.*, Science **309**, 1697 (2005).
[3] Y. Nambu, S. Nakatsuji, and Y. Maeno, J. Phys. Soc. Jpn. **75**, 043711 (2006).
[4] H. Takeya, K. Ishida, and K. Kitagawa *et al.* (unpublished); Meet. Abstr. Phys. Soc. Jpn. **62**, 476 (2007).
[5] H. Tsunetsugu and M. Arikawa, J. Phys. Soc. Jpn. **75**, 083701 (2006).
[6] A. Läuchli, F. Mila, and K. Penc, Phys. Rev. Lett. **97**, 087205 (2006).
[7] S. Bhattacharjee, V. B. Shenoy, and T. Senthil, Phys. Rev. B **74**, 092406 (2006).
[8] P. Li, G. M. Zhang, and S. Q. Shen, Phys. Rev. B **75**, 104420 (2007).
[9] S. Fujimoto, Phys. Rev. B **73**, 184401 (2006).
[10] H. Kawamura and A. Yamamoto, J. Phys. Soc. Jpn. **76**, 073704 (2007).
[11] K. Onuma, Y. Nambu, S. Nakatsuji, O. Sakai, and Y. Maeno (unpublished).
[12] L. Dogguy-Smiri, N. H. Dung, and M. P. Pardo, Mater. Res. Bull. **15**, 861 (1980).
[13] L. Dogguy-Smiri and N. H. Dung, Acta Crystallogr., B **38**, 372 (1982).
[14] K. Takada *et al.*, Nature (London) **422**, 53 (2003).
[15] W. Koshibae and S. Maekawa, Phys. Rev. Lett. **91**, 257003 (2003).
[16] J. Kanamori, J. Phys. Chem. Solids **10**, 87 (1959).
[17] I. Affleck *et al.*, Commun. Math. Phys. **115**, 477 (1988).